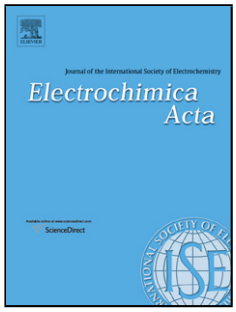

Title: Long-Range Hexagonal Arrangement of TiO_2 Nanotubes by Soft Lithography-Guided Anodization

Author: V. Vega J.M. Montero-Moreno J. García V.M. Prida W. Rahimi M. Waleczek C. Bae R. Zierold K. Nielsch

PII: S0013-4686(16)30804-0
DOI: http://dx.doi.org/doi:10.1016/j.electacta.2016.04.016
Reference: EA 27051

To appear in: *Electrochimica Acta*

Received date: 6-12-2015
Revised date: 3-4-2016
Accepted date: 5-4-2016

Please cite this article as: V.Vega, J.M.Montero-Moreno, J.García, V.M.Prida, W.Rahimi, M.Waleczek, C.Bae, R.Zierold, K.Nielsch, Long-Range Hexagonal Arrangement of TiO2 Nanotubes by Soft Lithography-Guided Anodization, Electrochimica Acta http://dx.doi.org/10.1016/j.electacta.2016.04.016

Long-Range Hexagonal Arrangement of TiO_2 Nanotubes by Soft Lithography-Guided Anodization

V. Vega[1], J. M. Montero-Moreno[2], J. García[1,2], V. M. Prida[1,*],W. Rahimi[2], M. Waleczek[2], C. Bae[3], R. Zierold[2], K. Nielsch[2]

[1]Departamento de Física, Universidad de Oviedo, Calvo Sotelo s/n, 33007-Oviedo, Spain
[2]Institute of Applied Physics, Universität Hamburg, Jungiusstr. 11, 20355-Hamburg, Germany
[3]Department of Energy Science, Sungkyunkwan University, Suwon 440-746, Korea

*Corresponding author:
Dr. Víctor M. Prida
Departamento de Física, Universidad de Oviedo.
Calvo Sotelo s/n, 33007-Oviedo, Asturias, Spain.
Telf.: 0034-985103294
Fax. 0034-985103324
e-mail: vmpp@uniovi.es

Graphical Abstract:

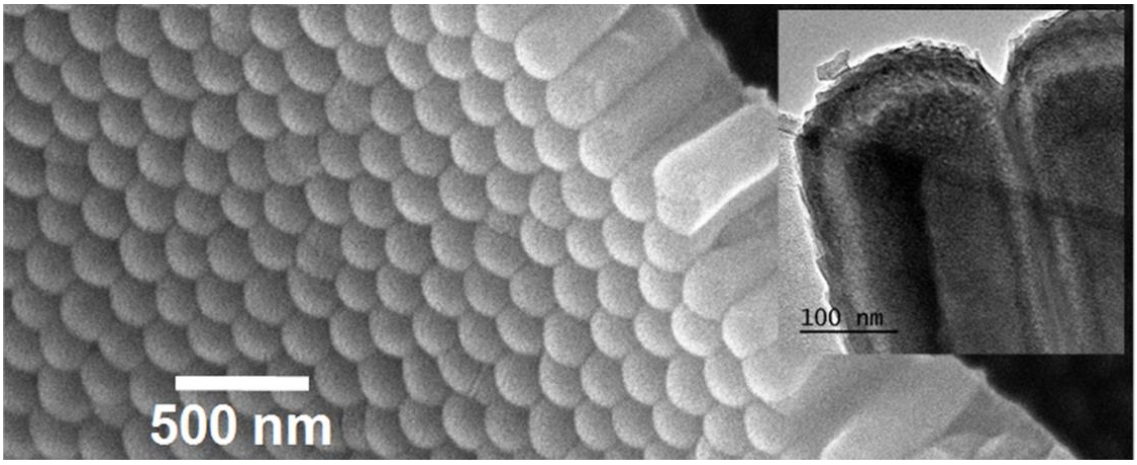

Scanning electron micrograph showing the highly hexagonally long-range ordering of the TiO_2 nanotubes array after following combined steps of Laser Interference Lithography pre-patterning and further electrochemical anodization procedure. Upper inset displays the TEM cross-section view of a pair of freestanding TiO_2 nanotubes, where it can be appreciated their dimensions.

Research Highlights:

- A novel strategy based on combined methods of Laser Interference Lithography and electrochemical anodization is developed for the fabrication of nanostructures.
- As a proof of concept, the synthesis of long-range hexagonally ordered TiO_2 nanotube arrays is demonstrated.
- TiO_2 nanotubes having 32 nm of inner diameter, around of 25 nm in wall thickness and 210 nm of lattice parameter were anodically grown under proper synthesis conditions.

ABSTRACT

Long range hexagonally ordered TiO_2 nanotube arrangements have been synthesized by employing a novel strategy consisted of combining the well-known Laser Interference Lithography technique together with electrochemical anodization methods. By properly tuning the fabrication parameters that make match between both techniques, TiO_2 nanotube arrays having near 32 nm of inner diameter, wall thickness around of 25 nm and 210 nm of lattice parameter were anodically grown on pre-patterned Ti foils over large sample surface areas, typically of several squared centimetres in size. This opens the possibility to the development of new types of functional devices based on self-organized morphologies of anodic TiO_2 nanotubes, requiring both high spatially ordered and defect-free nanotube arrangements.

Keywords: TiO_2 nanotubes, electrochemical anodization, laser interference lithography, self-assembling.

1. Introduction

During the last decade, TiO_2 nanotubes have received great attention in several research fields due to their unique tubular geometry together the exciting electronic and photochemical features exhibited by this oxide. The excellent biocompatibility [1], chemical and mechanical robustness [2-4], wide energy band gap [5], large specific surface area together with high catalytic and photocatalytic activities [6] exhibited by this multifunctional material make TiO_2 nanotubes useful for a wide range of applications, covering from dye-sensitized solar cells [7-10], water splitting for H_2 production [11-15], photocatalytic decomposition of hazardous wastes [16-19], gas sensors [20-23], drug delivery [24] and orthopaedic prosthesis [25, 26], or inclusive for magnetics and diluted magnetic semiconductors [27, 28], among others. Novel synthesis strategies couple titania nanoparticles or nanotubes to 1D photonic crystals of titania nanotube and found a significant increase of the power conversion efficiency of dye-sensitize solar cells [29, 30]. Also matching the surface plasmon resonance wavelength of gold nanoparticles to the photonic band gap of a titania nanotube film resulted in an enhancement of the photoelectrochemical water splitting performance [14, 31].

The origin of the excellent physicochemical properties of TiO_2 nanotubes, and particularly of its unusual photocatalytic activity is not well fully understood. There is a controversy on whether the geometrical structure or the crystalline nanotexture of the nanotubes prevail. Liu et al. showed, based on a theoretical kinetic model, that the geometrical parameters of TiO_2 nanotube arrays (tube length, inner diameter and tube wall) have a strong impact on their photocatalytic activity [32]. Other studies point out that the crystallographic facets exposed in the nanotubes wall significantly affect their photocatalytic and photochemical properties. In particular, the enhancement of the presence of the more reactive {001} crystal facets of anatase respect to the more thermodynamically stable {101} facets is demonstrated in such nanostructures, with improvement of the performance of TiO_2-based solar cells or in the photocatalytic decomposition of waste materials [33, 34].

The possibility of synthesizing films of self-aligned TiO_2 nanotubes displaying a rather uniform and well controlled geometry by means of the inexpensive and flexible electrochemical anodic oxidation method, i.e. titanium anodization [5, 35-38] has made this material widely accessible and applicable in many fields. Furthermore, continuous and increasing research efforts have allowed a deep understanding on the electrochemistry and mechanism of TiO_2 nanotubes growth [39-45], thus enabling a high control degree on the geometrical parameters of the resulting nanotubular anodic titanium oxides [5, 15, 46-49].

Thus, in the last years, there is an increasing interest in the development of TiO_2 nanotubes with superior uniformity of the geometrical and crystallographic parameters, coupling different properties as respects to their photocatalytic, photonic and electronic properties in order to obtain significant enhancements of the efficiency of TiO_2-based devices [50]. The investigation of novel synthesis strategies based on electrochemical anodization of Ti and allowing for an improvement of the uniformity and control degree of the nanotubes morphology, namely their diameter, wall thickness and spatial periodicity, over large surface areas can enhance the performance of current applications of TiO_2 nanotubes and may also give rise to novel uses of this highly functional material [51]. In this regard, a two-step anodization process has been employed in order to enhance the ordering degree of the TiO_2 nanotube array [52, 53]. This method, based on the spontaneous nanotubes self-ordered growth during the anodic oxidation of Ti, allows for an improvement of the spatial arrangement of the resulting nanotubes, despite the fact that a long-range hexagonal ordering of the nanotubes was not achieved by this technique. The use of high purity starting Ti foils has also been demonstrated to exert a strong impact on the final hexagonal arrangement of the TiO_2 nanotubes grown by the two-step anodization method [52].

Alternatively, Focused Ion Beam (FIB) has also been employed to define a hexagonal array of nanometric concavities on the surface of a Ti substrate, which act as seeds for the nucleation of TiO_2 nanotubes in a further anodization step [54, 55]. By this guided self-assembly method, an almost perfect hexagonal geometry was obtained in the TiO_2 nanotube arrays. However, the limitation in the maximum areas that can be effectively patterned by FIB (of only few squared microns in size) and the expensiveness of this technique make it not suitable for practical applications [56]. On the other hand, nanoimprinting of Ti by using metallic molds allows a high-throughput formation of ideally ordered pretexturing patterns that can generate highly ordered porous or nanotubular TiO_2 over a large sample area by adopting appropriate anodizing conditions [57].

In this work, we report on a novel combination of Laser Interference Lithography (LIL) and electrochemical anodization techniques that allows for guiding the spatially ordered growth of TiO_2 nanotubes arranged over large surface areas. This combined approach has been effectively demonstrated in the case of Al_2O_3 nanoporous films grown by the aluminum anodization technique in a previous work [58], and it is now adapted to anodic titania nanotube films as a proof of concept of the flexibility and suitability of this combination of nanofabrication techniques. Briefly, the process involves the use of LIL to pattern a photoresist layer with a highly regular hexagonal pattern of holes using a three-beam configuration [59].

The interpore distance is here the main parameter to control. Next the periodic structure is fully transferred into a second layer of SiO_2, which will work as a hard mask during the first stages of the anodization. A clean titanium surface is hence exposed at the bottom of the holes generated in the SiO_2 layer. During the subsequent anodization process, the hard mask forces the nucleation of the pores at the desired positions, resulting in a perfectly-ordered cellular array of TiO_2 nanotubes grown over large surface areas. It also prevents the oxide dissolution, which usually takes place at the cell junctions of the fluoride-rich layer typical of titanium anodization processes, assuring the coalescence of the whole structure [60]. The formation of a periodically ordered and high aspect ratio nanotube arrangement within TiO_2 could be achieved by properly tuning the more appropriate anodizing conditions for the nanotubes growth. These combined processes allow for the fabrication of hexagonally ordered TiO_2 nanotubes over a large area of the sample surface, thus enabling the expansion of the application fields of research for the anodized TiO_2 nanotube arrays requiring high spatially ordered and defect-free tube arrangements.

2. Experimental

Disc shaped high purity Ti foils (99.6 +%, Goodfellow, 2.5 cm in diameter) were mechanically polished up to a mirror-like finishing. The Ti substrates were then cleaned by ultrasonication in acetone, isopropanol and ethanol. Some of the polished substrates were directly anodized at room temperature (20 ± 2 ºC) in ethylene glycol based electrolytes containing 0.3 wt.% of NH_4F and 1.8 wt.% of H_2O, without any pre-patterning step, at several anodization voltages ranging between 30 V and 120 V.

A second batch of polished Ti substrates were lithographically patterned by means of a Laser Interference Lithography (LIL) setup described in detail elsewhere [58]. The layer stack employed for the LIL patterning is schematized in Figure 1 (a) and it consists of a SiO_2 protective layer deposited by means of sputtering (30 nm) and two spin-coated layers: a 70 nm of antireflection coating (DUV 112 from Brewer Science), together with a 200 nm of a high resolution positive photoresist (UV2000 from Microresist Technology). The hexagonal pattern was produced in a single exposure by using a 266 nm of wavelength CW laser, in a 3-beam configuration LIL setup and controlling the energy dose. The 3-beam LIL setup is based on the work of de Boor et al. [59], and consists of two mirrors, placed at an angle of 120 º to each other, being both perpendicular to the sample plane. In this setup, the three incident waves (direct laser beam and two reflected waves) have wave vectors with 120º symmetry, leading to the hexagonal pattern of dots onto the sample surface. After the laser beam exposure, the photoresist layer was developed employing an alkaline solution to reveal the photo-

lithographically printed hexagonal pattern in the photoresist layer. Afterwards, the pattern was transferred to the Ti substrate by a combination of Reactive Ion Etching (RIE) steps. Firstly, an O_2 plasma (25 mTor, 25 sccm, 75 W) was employed to transfer the hexagonal pattern to the organic ARC layer. Secondly, a CHF_3 plasma (transfers it in the SiO_2 layer and exposes in these sites the Ti substrate. Finally, the sample is exposed again to an O_2 plasma etching to remove the remaining organic coatings.

The patterned samples were then anodized in a potentiostatic mode at room temperature under the appropriated conditions (80 V) in vigorously stirred ethylene glycol electrolytes containing 0.3 wt.% of NH_4F and 1.8 wt.% of H_2O. The duration of the anodization process was adjusted to 300 s, similar to that reported in previous works on FIB-guided Ti anodization [54].

The TiO_2 nanotube arrays have been studied by electron microscopy techniques. Scanning Electron Microscopy (SEM) was performed in a JEOL-6610LV, equipped with an X-Ray Energy Dispersive Spectrometer (EDS). Prior to SEM characterization, the samples were coated with a thin Au layer, deposited by means of a Polaron 7620 Sputter coater, which enhances the electrical conductivity of the samples and improves the topographic contrast. Transmission Electron Microscopy (TEM) was performed in a JEOL-JEM 2100F microscope after releasing the TiO_2 nanotubes from the Ti substrates by mechanical scratching their surface with a scalpel. Selected Area Electron Diffraction (SAED) analyses performed with the high-resolution TEM were carried out to check the structure of the as-obtained anodic TiO_2 nanotubes and after thermal annealing treatments, and Scanning Transmission Electron Microscope (STEM) mode was also employed for the chemical composition analysis.

3. Results and discussion

Our guided self-assembly nanofabrication approach, which is schematically shown in Figure 1, is based on the LIL patterning of a SiO_2 layer with a 2D regular array of holes with hexagonal packing symmetry on a mechanically polished Ti foil of about 5 cm^2 in area, which can easily be extended to around 20 cm^2 [58]. The substrate is firstly coated with a uniform SiO_2 layer, followed by a suitable antireflection coating and a photoresist sensitive to the 266 nm laser, both deposited by spin coating (Fig. 1(a)). A combination of selective dry-etching steps, performed by Reactive Ion Etching (RIE), is then employed to successfully transfer the pattern onto the sacrificial passivating SiO_2 layer (Fig. 1(b). Further step, the titanium samples are anodized at constant voltage and under proper conditions to create the TiO_2 nanotube arrangement (Fig 1(c)).

TiO_2 nanotubes are formed by electrochemical anodization of Ti in fluoride containing electrolytes. Upon the application of an anodic voltage, Ti is oxidized to Ti^{4+} and reacts with O^{2-} ions to form a compact layer of titanium oxide leading to surface passivation of the Ti anode. The role of fluoride ions is a key factor for the development of the nanotubular structure of the oxide layer, due to the formation of water soluble titanium hexafluoride species, thus enabling a competition between the oxidation and field-enhanced dissolution of oxide at the bottom of nanotubes. This mechanism allows for a continuous growth of the TiO_2 nanotubes [5, 60]. Additionally, the F^- ions migrate inwards through the barrier oxide layer of nanotubes at a faster rate than O^{2-} ions, giving rise to the formation of a fluoride-rich titania layer at the metal-oxide interface that separates the nanotube bases from the Ti substrate. As the growth of the TiO_2 nanotubes film continues, the fluoride-rich material is incorporated into the cell walls at the boundaries between adjacent-nanotubes.

The lower chemical resistance of this fluoride-rich layer causes its preferential dissolution in acidic media giving rise to the segregation of the nanotubes [2, 5]. The morphology and size of the TiO_2 nanotubes is strongly affected by the electrochemical conditions employed in the anodization procedure, including pH and water content of the electrolyte, applied voltage and temperature, among other parameters [37, 39-46,45 48, 51, 60].

In order to determine the optimum electrochemical conditions that guarantee the perfect matching between the geometrical parameters of the LIL pattern with those of the nanotubes grown by electrochemical anodization, a series of polished Ti substrates without any pre-patterning step were anodized at room temperature in ethylene glycol based electrolyte containing NH_4F and H_2O, at several anodization voltages ranging from 30 V to 120 V. Figure 2 shows selected SEM images of the top (a-c) and bottom (d-f) sides of some of the resulting layers formed by anodic TiO_2 nanotubes, whereas Figure 3 depicts the average distance among adjacent nanotubes, obtained by image analysis of the bottom-view SEM images of samples. A quasi-linear increase of the average inter-tube distance with the anodization voltage can be observed for samples anodized at constant voltages ranging between 30 and 80 V, with a slope of 2.8 nm/V [45]. In this voltage interval, the sample surface shows a highly compact nanotubular structure, with a porous-like layer covering the top-surface of the nanotubes. This layer remains from the initial compact oxide layer formed in the early stages of the anodization and is not dissolved due to the limited dissolution of TiO_2 in organic electrolytes [60]. When the anodization potential exceeds a critical value, of around 80-90 V, a transition from compact nanotubes to segregated nanotube morphology is found, and it is accompanied by a decrease in the average inter-tube distance, in good agreement with previous works [51, 60], which is related to water dissociation and oxide dissolution, being both enhanced by the effect of the electric field. From the above discussion, a broad window of inter-tube distances from 80 nm up to 220 nm is available by employing this electrolytic bath, while keeping compact nanotubular structures and good control on the average inter-tube distance.

As regards to our LIL setup, by using a 266 nm deep-UV laser and the 3-beam configuration, a broad window of interhole distances in the SiO_2 layer between 190 nm and 525 nm is experimentally available [58]. Shorter interhole distances are difficult to realize using this setup. However, LIL setups using the 195 nm line or other techniques like achromatic interference lithography could be used if smaller interhole distances are desired. Thus, a narrow overlapping between the window of interhole distances available by our LIL system and the window of inter-tube distances available by our anodization setup goes from 190 nm up to 220 nm. We selected a value of 210 nm to demonstrate this approach, which corresponds to an anodization voltage of 80 V, which corresponds to the first value of the anodic voltage at which the segregated nanotubes formation is observed.

A comparison between the current density transients obtained during the electrochemical anodization at 80 V of both, the as-polished Ti foil and LIL patterned Ti foil, is shown in Figure 4. Both curves display similar behavior, with a large decrease of the anodic current density during the first seconds of the process, followed by a recovery and stabilization of the anodic current, associated with a steady state of oxidation-dissolution equilibrium, leading to TiO_2 nanotubes growth. The main difference between both plots is the reduced value of the anodic current density obtained during the anodization of LIL-patterned Ti substrates, which is due to the SiO_2 template layer that limits the anodic oxidation of Ti, resulting also in a reduction of the nanotubes growth rate.

The morphology of the resulting TiO_2 nanotubes was studied by SEM, as it is displayed in Figure 5. Fig. 5 (a) corresponds to a top view of a highly ordered TiO_2 nanotube array synthesized in the above-mentioned conditions. It can be observed that the nucleation of the nanotubes takes place in the sites or holes defined by the LIL pattern. The bottom surface of the nanotube arrays can be observed in Figures 5 (b) and (d). The high magnification micrograph shown in Fig. 5 (b) demonstrates the existence of wide regions displaying a perfectly ordered hexagonal arrangement of TiO_2 nanotubes. However, the SEM image of Fig. 5 (d), which has been taken at lower magnification, evidences the existence of local defects in the hexagonal arrangement of TiO_2 nanotubes that can be related to both, isolated surface defects in the patterned Ti surface and nucleation faults occurred during the early stages of the anodization process. Nevertheless, these local defects do not affect the overall, long-range hexagonal ordering of the TiO_2 nanotubes array, as can be confirmed in the inset of Fig. 5 (d) that corresponds to a Fast Fourier Transform (FFT) of the respective image, which evidences the highly hexagonal symmetry of the nanotubes array. It is worth to mention that the SiO_2 layer not only serves to define the pore nucleation sites, but also hinders the dissolution of the fluoride-rich TiO_2 layer that takes place at the cell boundaries during the anodization, originating the nanotubular-like morphology exhibited in Fig. 2 (c), and resulting in a more mechanically stable TiO_2 layer [4].

The chemical analysis of the highly ordered nanotube arrays displayed in the Figure 6 that was performed by Electron Dispersive X-ray Spectroscopy (EDS) with the SEM, evidences the TiO_2 composition of the anodically patterned Ti samples. The presence of carbon impurities coming from the electrolyte (probably from the ethylene glycol) is also detected. Furthermore, the incorporation of small amounts of fluoride ions into the nanotubes during the anodization process is also confirmed in the EDS spectrum.

High Resolution Transmission Electron Microscopy (HR-TEM), together with Selected Area Electron Diffraction (SAED), were employed to characterize the morphology and crystalline structure of TiO_2 nanotubes, as shown in Fig. 7. This study was performed on TiO_2 nanotubes grown by anodic oxidation of mechanically polished Ti substrates (a, b and c), and also for the LIL pre-patterned Ti substrates (d, e and f), respectively. The TEM micrographs shown in Fig. 7 a) and d) correspond to a cross-section view of freestanding TiO_2 nanotubes, and the SAED spectra shown in their respective insets evidence that no crystalline structure can be found in the HR-TEM analysis, due to they exhibit a typical amorphous halo in both cases. Figures 7 b) and e) correspond to a comparison between the top view TEM images of the TiO_2 nanotube arrays. In a closer view, the STEM micrographs displayed in Figs. 7 c) and f) show the respective high magnifications of the mechanically polished and LIL pre-patterned anodic TiO_2 nanotubes, where it can be evidenced the existence of a three-layer morphology in both kind of structures. According with previous works by Albu et al., [2] each layer can be assigned to the electrolyte richly contaminated layer (close to the pore, at the center of the nanostructure), the electrolyte poorly contaminated layer and the F-rich layer (at the cell boundaries). From these two figures, it can be seen that the TiO_2 nanotubes form a compact structure with the F-rich layer at the cell boundaries as bright regions.

The TiO_2 nanotube samples were further thermal annealed at 400 °C for 3 hours in air. The resulting crystalline structure formed under these standard conditions is shown in Fig. 8 a) to c) for the mechanically polished anodic TiO_2 nanotubes and Fig. 8 d) to f) for the LIL pre-patterned anodic TiO_2 nanotubes, respectively. The HR-TEM images show a nanocrystalline morphology in both disordered and ordered samples, with a wide distribution of grain sizes. Both samples contain nanocrystals in size below 10 nm, while nanocrystals larger than 30 nm have also been identified. The more thermodynamically stable facets {101} displayed in Figs. 8 c) and f) have been identified in the large crystals present in both, ordered and disordered samples. The insets displayed in the Figs 8 b) and e) show the respective SAED spectra of the annealed TiO_2 nanotubes. Well-defined rings around the center beam ratify the polycrystalline morphology. These can be clearly assigned to anatase phase. The presence of rutile phase is not evidenced by the SAED spectra from HR-TEM analysis. In addition, the multilayered structure observed in the as-prepared samples becomes not evident after the annealing, which is in agreement with the loss of C and F after this process [2, 60].

4. Conclusions

The controlled growth of highly ordered geometrical structures of TiO_2 nanotubes can be tailored by employing the LIL technique through the pretexturing of Ti with a photoresist layer by properly tuning the fabrication parameters, having a highly hexagonal arrangement of holes with a well-defined interpores distance and transferring this designed regular pattern to the nanotubes growth under the subsequent anodization process. Our results demonstrate that the combined employment of these fabrication strategies allows for the nucleation of the pores at the desired positions, resulting in an ideally ordered cellular array of TiO_2 nanotubes extended over a large area of the sample surface, in the range of several squared centimeters. The highly ordered arrays of TiO_2 nanotubes growth exhibit a regular hexagonally centered

geometry having an average inner diameter of 32 ± 7 nm, around of 25 ± 5 nm in wall thickness and 210 nm of lattice parameter. The chemical composition and crystallization features of the highly spatially ordered TiO_2 nanotube arrays here investigated are not affected by the pretexturing defined by LIL-guided anodization. Local defects associated to inhomogeneities generated during the LIL process together nanotubes nucleation steps may result in local faults in the spatial arrangement of the TiO_2 nanotubes. However, the large-scale hexagonal ordering of the TiO_2 nanotubes is not affected by these local defects and it spans over the entire sample surface, thus expanding significantly the types of functional devices that can be designed based on self-organized morphologies of anodized TiO_2 nanotubes, requiring both high spatially ordered and defect-free nanotube arrangements.

Acknowledgment

Spanish MINECO funds under research project Nº MAT2013-48054-C2-2-R, together Consejería de Economía y Empleo from Principado de Asturias and FICyT under project Nº GIC-FC-15-GRUPIN14-085, are gratefully acknowledged. V. Vega thanks to DAAD and University of Oviedo for the respective internship grants. Scientific and technical support from the Scientific-Technical Services of the University of Oviedo is also recognized.

References

[1] C. A. Grimes, G. K. Mor, "TiO_2 Nanotube Arrays: Synthesis, Properties, and Applications", Ch. 6, "Use of TiO_2 Nanotube Arrays for Biological Applications", Springer Science & Business Media, LLC (2009), DOI 10.1007/978-1-4419-0068-5_6.

[2] S. P. Albu, A. Ghicov, S. Aldabergenova, P. Drechsel, D. LeClere, G. E. Thompson, J. M. Macak, P. Schmuki, Formation of Double-Walled TiO_2 Nanotubes and Robust Anatase Membranes, Adv. Mater. 20 (2008) 4135-4139.

[3] M. Paulose, L. Peng, K. C. Popat, O. K. Varghese, T. J. LaTempa, N. Bao, T. A. Desai, C. A. Grimes, Fabrication of mechanically robust, large area, polycrystalline nanotubular/porous TiO_2 membranes, J. Membrane Sci. 319 (2008) 199-205.

[4] T. Shokuhfar, G. K. Arumugam, P. A. Heiden, R. S. Yassar, C. Friedrich, Direct Compressive Measurements of Individual Titanium Dioxide Nanotubes, ACS Nano 3 (2009) 3098-3102.

[5] P. Roy, S. Berger, P. Schmuki, TiO_2 Nanotubes: Synthesis and Applications, Angew. Chem. Int. Ed. 50 (2011) 2904-2939.

[6] J. Lin, X. Liu, S. Zhu, Y. Liu, X. Chen, Anatase TiO_2 nanotube powder film with high crystallinity for enhanced photocatalytic performance, Nanoscale Res. Lett. 10 (2015) 110.

[7] B. O'Regan, M. Grätzel, A Low-Cost, High-Efficiency Solar Cell Based on Dye- sensitized Colloidal TiO_2 Films, Nature 353 (1991) 737-740.

[8] M. Paulose, K. Shankar, O.K. Varghese, G. K. Mor, C.A. Grimes, Application of highly-ordered TiO_2 nanotube-arrays in heterojunction dye-sensitized solar cells, J. Phys. D: Appl. Phys. 39 (2006) 2498–2503.

[9] T. Stergiopoulos, A. Ghicov, V. Likodimos, D.S. Tsoukleris, J. Kunze, P. Schmuki, P. Falaras, Dye-sensitized solar cells based on thick highly ordered TiO_2 nanotubes produced by controlled anodic oxidation in non-aqueous electrolytic media, Nanotechnology 19 (2008) 235602.

[10] P. V. Kamat, TiO_2 Nanostructures: Recent Physical Chemistry Advances, J. Phys. Chem. C 116 (2012) 11849–11851.

[11] J. H. Park, S. Kim, A. J. Bard, Novel Carbon-Doped TiO_2 Nanotube Arrays with High Aspect Ratios for Efficient Solar Water Splitting, Nano Lett. 6 (2006) 24-28.

[12] G. Wang, H. Wang, Y. Ling, Y. Tang, X. Yang, R. C. Fitzmorris, C. Wang, J. Z. Zhang, Y. Li, Hydrogen-Treated TiO_2 Nanowire Arrays for Photoelectrochemical Water Splitting, Nano Lett. 11 (2011) 3026-3033.

[13] S. Liang, J. He, Z. Sun, Q. Liu, Y. Jiang, H. Cheng, B. He, Z. Xie, S. Wei, Improving Photoelectrochemical Water Splitting Activity of TiO_2 Nanotube Arrays by Tuning Geometrical Parameters, J. Phys. Chem. C 116 (2012) 9049-9053.
[14] Z. Zhang, L. Zhang, M. N. Hedhili, H. Zhang, P. Wang, Plasmonic Gold Nanocrystals Coupled with Photonic Crystal Seamlessly on TiO_2 Nanotube Photoelectrodes for Efficient Visible Light Photoelectrochemical Water Splitting, Nano Lett. 13 (2013) 14-20.
[15] A. M. Mohamed, A. S. Aljaber, S. Y. Alqaradawi, N. K. Allam, TiO_2 nanotubes with ultrathin walls for enhanced water splitting, Chem. Commun. 51 (2015) 12617-12620.
[16] M. Zlamal, J. M. Macak, P. Schmuki, J. Krysa, Electrochemically assisted photocatalysis on self-organized TiO_2 nanotubes, Electrochem. Commun. 9 (2007) 2822–2826.
[17] M. N. Chong, B. Jin, C. W. K. Chow, C. Saint, Recent developments in photocatalytic water treatment technology: a review, Water Res. 44 (2010) 2997-3027.
[18] Y. Hou, X. Li, Q. Zhao, X. Quan, G. Chen, Electrochemically Assisted Photocatalytic Degradation of 4-Chlorophenol by $ZnFe_2O_4$-Modified TiO_2 Nanotube Array Electrode under Visible Light Irradiation, Environ. Sci. Technol. 44 (2010) 5098-5103.
[19] S. Ozkan, A. Mazare, P. Schmuki, Extracting the limiting factors in photocurrent measurements on TiO_2 nanotubes and enhancing the photoelectrochemical properties by Nb doping, Electrochim. Acta 176 (2015) 819-826.
[20] G. K. Mor, M. A. Carvalho, O. K. Varghese, M. V. Pishko, C. A. Grimes, A room-temperature TiO_2-nanotube hydrogen sensor able to self-clean photoactively from environmental contamination, J. Mater. Res. 19 (2004) 628-634.
[21] H. F. Lu, F. Li, G. Liu, Z.-G. Chen, D.-W. Wang, H.-T. Fang, G. Q. Lu, Z. H. Jiang, H.-M. Cheng, Amorphous TiO_2 nanotube arrays for low-temperature oxygen sensors, Nanotechnology 19 (2008) 405504.
[22] Y. Li, X. Yu, Q. Yang, Fabrication of TiO_2 Nanotube Thin Films and Their Gas Sensing Properties, Journal of Sensors (2009) ID 402174.
[23] X. Zhang, J. Zhang, Y. Jia, P. Xiao, J. Tang, TiO_2 Nanotube Array Sensor for Detecting the SF_6 Decomposition Product SO_2, Sensors 12 (2012) 3302-3313.
[24] D. Losic, M. S. Aw, A. Santos, K. Gulati, M. Bariana, Titania Nanotube Arrays for Local Drug Delivery: Recent Advances and Perspectives, Expert Opinion on Drug Delivery 12 (2014) 103-127.
[25] K. S. Brammer, C. J. Frandsen, S. Jin, TiO_2 nanotubes for bone regeneration, Trends in Biotechnology 30 (2012) 315-322.

[26] P. Neacsu, A. Mazare, P. Schmuki, A. Cimpean, Attenuation of the macrophage inflammatory activity by TiO_2 nanotubes via inhibition of MAPK and NF-κB pathways, International Journal of Nanomedicine 10 (2015) 6455-6467.
[27] V. M. Prida, M. Hernández-Vélez, M. Cervera, K. Pirota, R. Sanz, D. Navas, A. Asenjo, P. Aranda, E. Ruiz-Hitzky, F. Batallán, M. Vaázquez, B. Hernando, A. Menéndez, N. Bordel, R. Pereiro, Magnetic behaviour of arrays of Ni nanowires by electrodeposition into self-aligned titania nanotubes, J. Magn. Magn. Mater. 294 (2005) e69-e72.
[28] V. M. Prida, M. Hernández-Vélez, K. R. Pirota, A. Menéndez, M. Vázquez, Synthesis and magnetic properties of Ni nanocylinders in self-aligned and randomly disordered grown titania nanotubes, Nanotechnology 16 (2005) 2696.
[29] C. T. Yip, H. Huang, L. Zhou, K. Xie, Y. Wang, T. Feng, J. Li, W. Y. Tam, Direct and Seamless Coupling of TiO_2 Nanotube Photonic Crystal to Dye-Sensitized Solar Cell: A Single-Step Approach, Adv. Mater. 23 (2011) 5624-5628.
[30] M. Guo, K. Xie, J. Lin, Z. Yong, C. T. Yip, L. Zhou, Y. Wang, H. Huang, Design and coupling of multifunctional TiO_2 nanotube photonic crystal to nanocrystalline titania layer as semi-transparent photoanode for dye-sensitized solar cell, Energy Environ. Sci. 5 (2012) 9881-9888.
[31] N. T. Nguyen, M. Altomare, J. E. Yoo, P. Schmuki, Efficient Photocatalytic H_2 Evolution: Controlled Dewetting–Dealloying to Fabricate Site-Selective High-Activity Nanoporous Au Particles on Highly Ordered TiO_2 Nanotube Arrays, Adv. Mater. 27 (2015) 3208-3215.
[32] B. Liu, K. Nakata, S. Liu, M. Sakai, T. Ochiai, T. Murakami, K. Takagi, A. Fujishima, Theoretical Kinetic Analysis of Heterogeneous Photocatalysis by TiO_2 Nanotube Arrays: the Effects of Nanotube Geometry on Photocatalytic Activity, J. Phys. Chem. C 116 (2012) 7471-7479.
[33] M.-H. Jung, K. C. Ko, J. Y. Lee, Single Crystalline-like TiO_2 Nanotube Fabrication with Dominant (001) Facets using Poly(vinylpyrrolidone), J. Phys. Chem. C 118 (2014) 17306-17317.
[34] M. Kim, C. Bae, H. Kim, H. Yoo, J. M. Montero-Moreno, H. S. Jung, J. Bachmann, K. Nielsch, H. Shin, Confined crystallization of anatase TiO_2 nanotubes and their implications on transport properties, J. Mater. Chem. A 1 (2013) 14080-14088.
[35] V. Zwilling, M. Aucoutuier, E. Darque-Ceretti, Anodic oxidation of titanium and TA6V alloy in chromic media. An electrochemical approach, Electrochim. Acta 45 (1999) 921-929.
[36] J. M. Macak, H. Tsuchiya, L. Taveira, S. Aldabergerova, P. Schmuki, Smooth Anodic TiO_2 nanotubes, Angew. Chem. Int. Ed. 44 (2005) 7463-7465.

[37] S. Bauer, S. Kleber, P. Schmuki, TiO_2 nanotubes: Tailoring the geometry in H_3PO_4/HF electrolytes, Electrochem. Commun. 8 (2006) 1321-1325.
[38] S. P. Albu, A. Ghicov , J. M. Macak , R. Hahn , P. Schmuki, Self-Organized, Free-Standing TiO_2 Nanotube Membrane for Flow-through Photocatalytic Applications, Nano Lett. 7 (2007) 1286-1289.
[39] V Vega, V. M. Prida, M. Hernández-Vélez, E. Manova, P. Aranda, E. Ruiz-Hitzky, M. Vázquez, Influence of Anodic Conditions on Self-ordered Growth of Highly Aligned Titanium Oxide Nanopores, Nanoscale Res Lett. 2 (2007) 355-363.
[40] V. M. Prida, E. Manova, V. Vega, M. Hernandez-Velez, P. Aranda, K. R. Pirota, M. Vázquez, E. Ruiz-Hitzky, Temperature Influence on the Anodic Growth of Self-Aligned Titanium Dioxide Nanotubes Arrays. J. Magn. Magn. Mater. 316 (2007) 110-113.
[41] V. Vega, M. A. Cerdeira, V. M. Prida, D. Alberts, N. Bordel, R. Pereiro, F. Mera, S. García, M. Hernández-Vélez, M. Vázquez, Electrolyte influence on the anodic synthesis of TiO_2 nanotube arrays, J. Non-Cryst. Solids 354 (2008) 5233-5235.
[42] S. P. Albu, P. Schmuki, Influence of anodization parameters on the expansion factor of TiO_2 nanotubes, Electrochim. Acta 91 (2013) 90-95.
[43] Y. Yang, Y. Li, M. Pritzker, Morphological evolution of anodic TiO_2 nanotubes, RSC Advances 4 (2014) 35833-35843.
[44] A. Apolinário , P. Quitério, C. T. Sousa, J. Ventura, J. B. Sousa, L. Andrade, A. M. Mendes, J. P. Araújo, Modeling the Growth Kinetics of Anodic TiO_2 Nanotubes, J. Phys. Chem. Lett. 6 (2015) 845-851.
[45] P. Quitério, A. Apolinário, C.T. Sousa, J. D. Costa, J. Ventura, J. P. Araújo, The cyclic nature of porosity in anodic TiO_2 nanotube arrays, J. Mater. Chem. A 3 (2015) 3692-3698.
[46] Y. Alivov, M. Pandikunta, S. Nikishin, Z. Y. Fan, The anodization voltage influence on the properties of TiO_2 nanotubes grown by electrochemical oxidation, Nanotechnology 20 (2009) 225602.
[47] H. Li, J.-W. Cheng, S. Shu, J. Zhang, L. Zheng, C. K. Tsang, H. Cheng, F. Liang, S.-T. Lee, Y. Y. Li, Selective Removal of the Outer Shells of Anodic TiO_2 Nanotubes, Small 9 (2013) 37-44.
[48] J. Kapusta-Kołodziej, O. Tynkevych, A. Pawlik, M. Jarosz, J. Mech, G. D. Sulka, Electrochemical growth of porous titanium dioxide in a glycerol-based electrolyte at different temperatures, Electrochim. Acta 144 (2014) 127-135.
[49] K. Gulati, A. Santos, D. Findlay, D. Losic, Optimizing Anodization Conditions for the Growth of Titania Nanotubes on Curved Surfaces, J. Phys. Chem. C 119 (2015) 16033-16045.

[50] A. Mazzarolo, K. Lee, A. Vicenzo, P. Schmuki, Anodic TiO_2 nanotubes: Influence of top morphology on their photocatalytic performance, Electrochem. Commun. 22 (2012) 162-165.
[51] Z. Su, W. Zhou, Pore diameter control in anodic titanium and aluminium oxides, J. Mater. Chem. 21 (2011) 357-362.
[52] J. M. Macak, S. P. Albu, P. Schmuki, Towards ideal hexagonal self-ordering of TiO_2 nanotubes, Phys. Stat. Solidi Rapid Res. Lett. 1 (2007) 181-183.
[53] Y. Shin, S. Lee, Self-Organized Regular Arrays of Anodic TiO_2 Nanotubes, Nano Lett. 8 (2008) 3171-3173.
[54] B. Chen, K. Lu, Z. Tian, Effects of titania nanotube distance and arrangement during focused ion beam guided anodization, J. Mater. Chem. 21 (2011) 8835-8840.
[55] B. Chen, K. Lu, Influence of Patterned Concave Depth and Surface Curvature on Anodization of Titania Nanotubes and Alumina Nanopores, Langmuir 27 (2011) 12179-12185.
[56] B Chen, K. Lu, Z. Tian, Novel Patterns by Focused Ion Beam Guided Anodization, Langmuir 27 (2011) 800-808.
[57] T. Kondo, S. Nagao, T. Yanagishita, N. T. Nguyen, K. Lee, P. Schmuki, H. Masuda, Ideally ordered porous TiO_2 prepared by anodization of pretextured Ti by nanoimprinting process, Electrochem. Commun. 50 (2015) 73-76.
[58] J. M. Montero-Moreno, M. Waleczek, S. Martens, R. Zierold, D. Görlitz, V. Vega Martínez, V. M. Prida, K. Nielsch, Constrained Order in Nanoporous Alumina with High Aspect Ratio: Smart Combination of Interference Lithography and Hard Anodization, Adv. Funct. Mater. 24 (2014) 1857-1863.
[59] J. de Boor, N. Geyer, U. Gösele, V. Schmidt, Three-beam interference lithography: upgrading a Lloyd's interferometer for single-exposure hexagonal patterning, Optics Letters 34 (2009) 1783-1785.
[60] D. Regonini, C. R. Bowen, A. Jaroenworaluck, R. Stevens, A Review of Growth Mechanism, Structure and Crystallinity of Anodized TiO_2 Nanotubes, Mater. Sci. & Eng. R – Reports 74 (2013) 377-406.

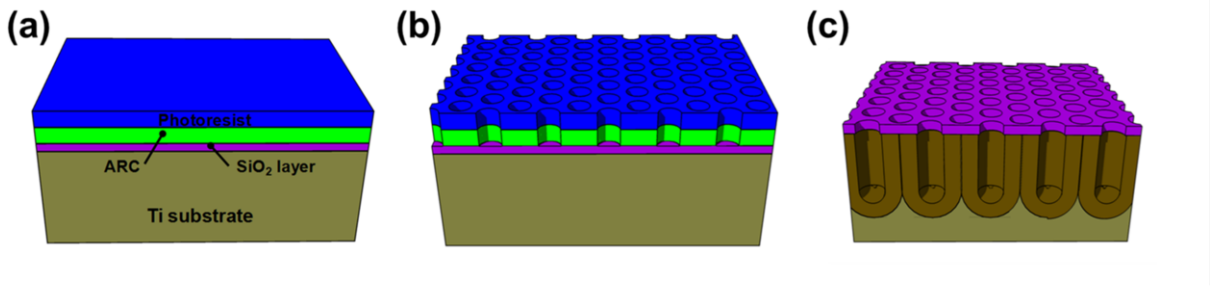

Figure 1: Schematic drawing of the procedure followed in the fabrication of the patterned Ti substrate employed for the guided self-assembly growth of highly ordered TiO_2 nanotube arrays. a) layer stack b) after LIL exposure and first plasma etching c) after second and third plasma etching and subsequent Ti anodization.

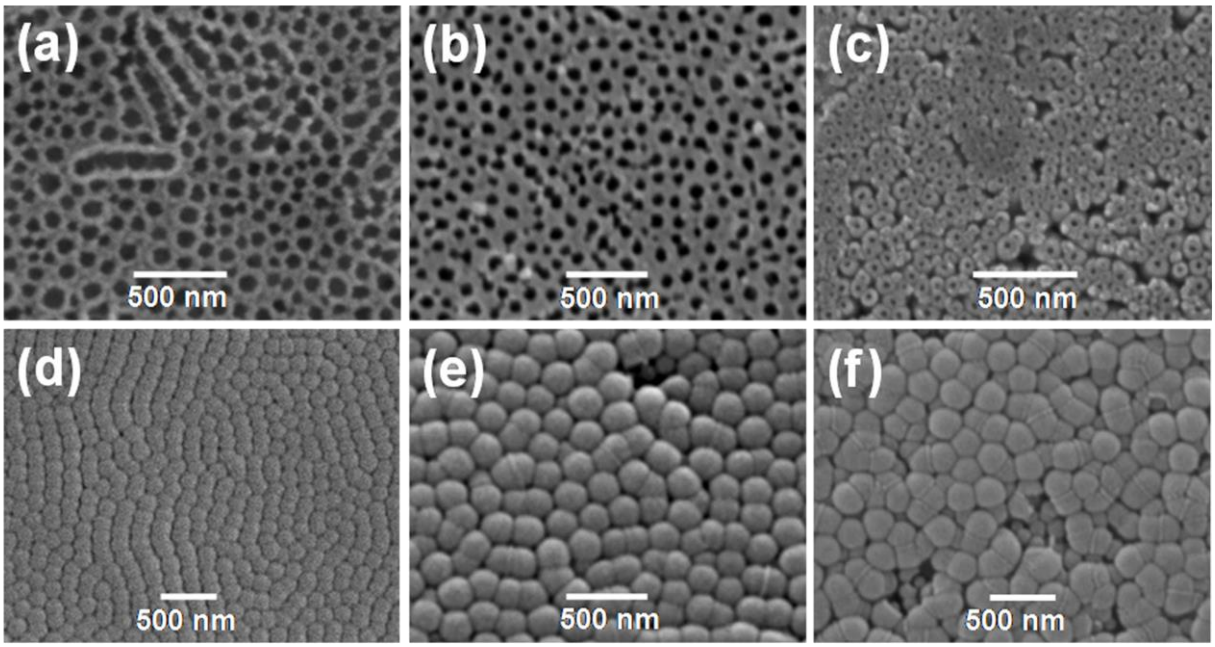

Figure 2: SEM top views (a-c) and bottom views (d-f) of TiO_2 nanotube arrays synthesized by electrochemical anodization of polished Ti substrates in ethylene glycol based electrolytes containing 0.3 wt.% of NH_4F and 1.8 wt.% of H_2O, without any pre-patterning step and at the anodization voltages of 60 V (a,d); 70 V (b, e) and 80 V (c, f), respectively.

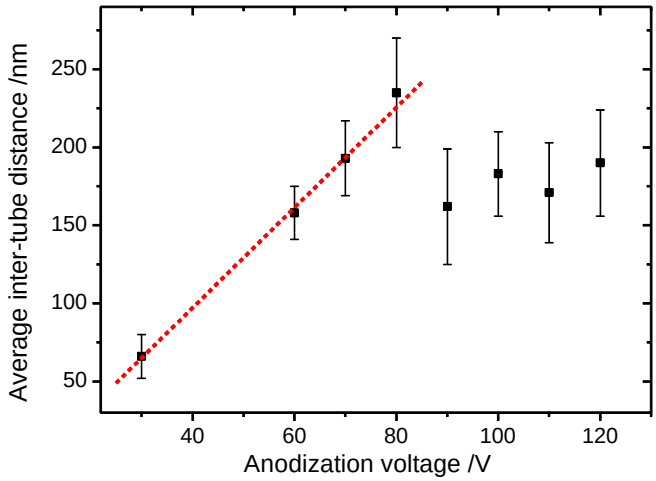

Figure 3: Dependence of the average distance among adjacent TiO_2 nanotubes on the anodization voltage. The region within the linear regime corresponds to the homogeneous nanotubes growth.

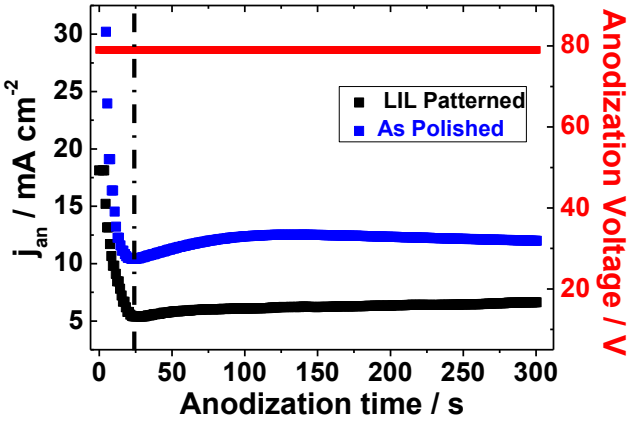

Figure 4: Current density transients recorded during the potentiostatic anodic oxidation performed at 80 V, for the as polished and LIL patterned Ti foils, respectively.

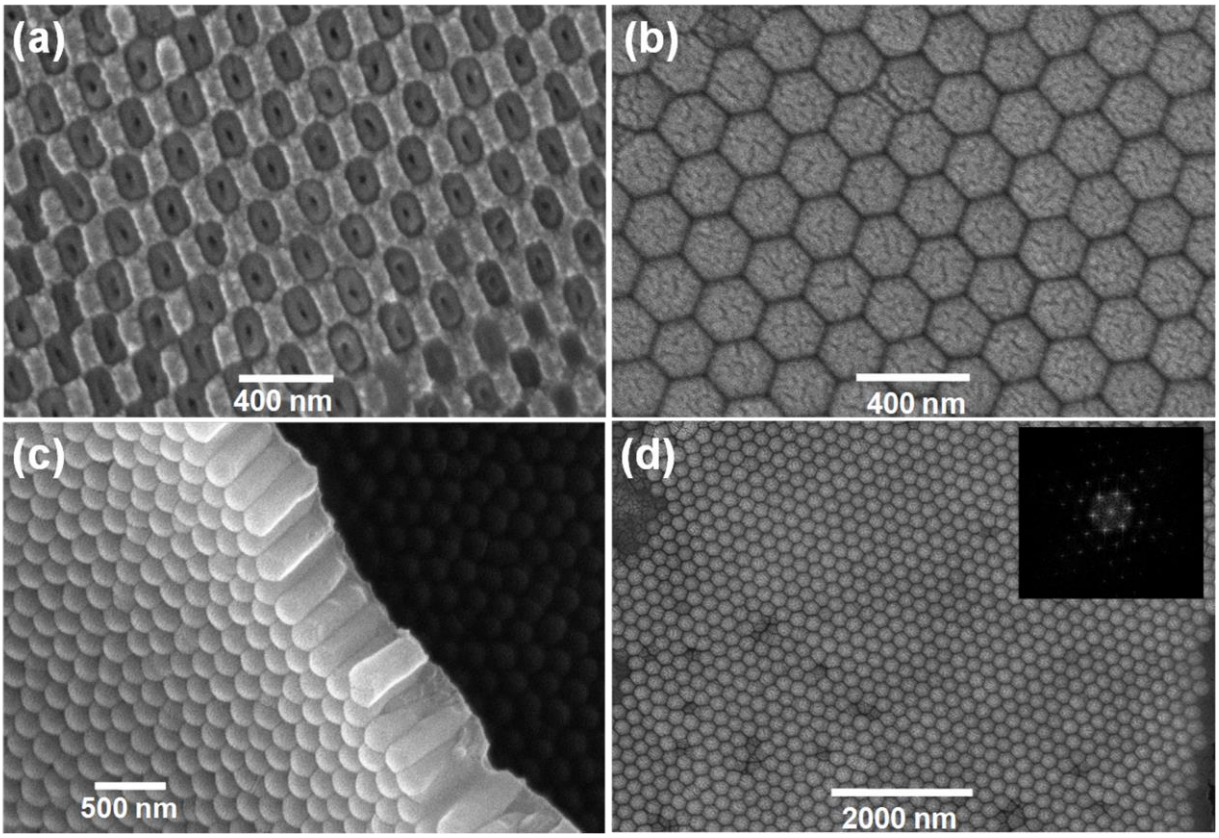

Figure 5: SEM images of highly hexagonally ordered TiO_2 nanotube arrays fabricated by LIL guided anodization. (a) Top view. (b) High magnification bottom view. (c) Cross-section view. (d) Low magnification bottom view. The inset shows a FFT of the image, evidencing the long-range high hexagonal ordering degree of the back-side of TiO_2 nanotubes array.

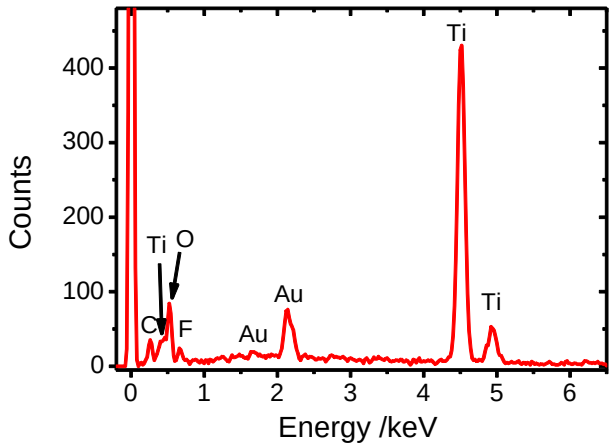

Figure 6: EDS spectra of a highly ordered nanotube array, evidencing the presence of Ti and O.

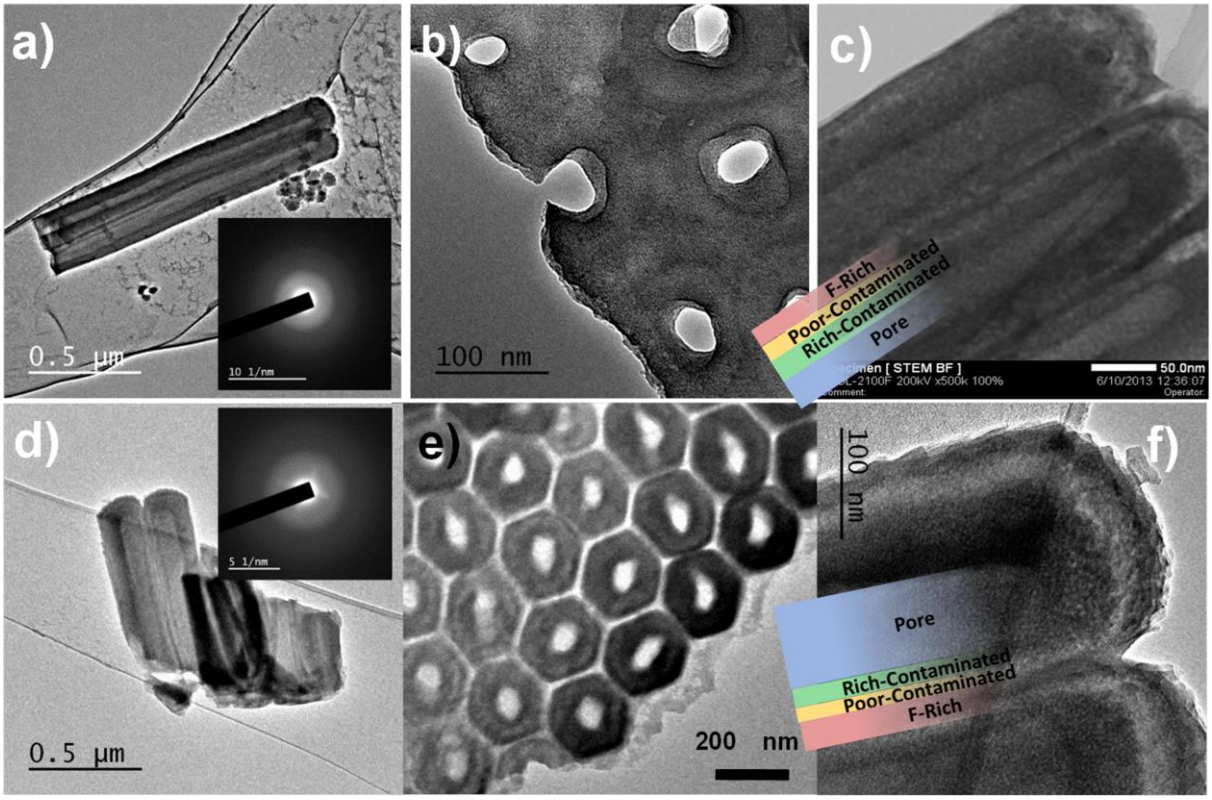

Figure 7: HR-TEM micrographs of TiO_2 nanotubes obtained by electrochemical anodization of mechanically polished (a, b and c) and LIL pre-patterned (d, e and f) Ti substrates, respectively. a) and d) show a cross section view of freestanding TiO_2 nanotubes, while b) and e) correspond to a top view of the nanotube arrays. The insets in a) and d) display the respective SAED spectra. The micrographs in c) and f) are the respective high magnifications of the mechanically polished and LIL pre-patterned anodic TiO_2 nanotubes, indicating the zones with different contamination of F across the nanotube walls.

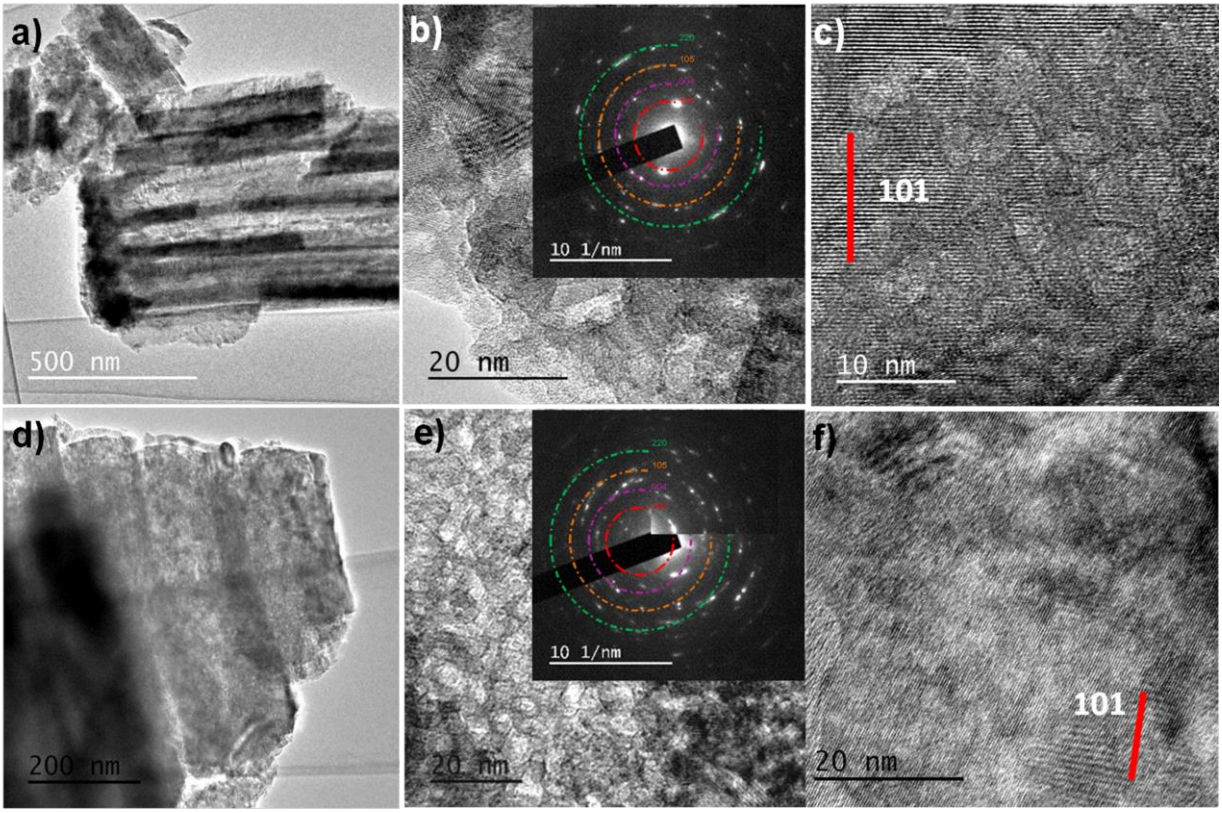

Figure 8: TiO_2 nanotube samples after being thermal annealed at 400 °C for 3 hours under air atmosphere. The resulting crystalline structure is shown in Figs. 8 a) to c) for the mechanically polished anodic TiO_2 nanotubes and Figs. 8 d) to f) for the LIL pre-patterned ones, respectively. The respective SAED spectra for the annealed TiO_2 nanotubes, shown as insets in b) and e), evidence the formation of anatase nanocrystals. In c) and f) the HR-TEM images display the {101} stable facets, corresponding to the large size crystals present in both, ordered and disordered samples.